

Accurate Evolution of Orbiting Binary Black Holes

Peter Diener,^{1,2} Frank Herrmann,^{3,4} Denis Pollney,³ Erik Schnetter,^{1,3} Edward Seidel,^{1,2,3} Ryoji Takahashi,¹
Jonathan Thornburg,³ and Jason Ventrella¹

¹*Center for Computation and Technology, Louisiana State University, Baton Rouge, Louisiana 70803, USA*

²*Department of Physics and Astronomy, Louisiana State University, Baton Rouge, Louisiana 70803, USA*

³*Max-Planck-Institut für Gravitationsphysik, Albert-Einstein-Institut, Am Mühlenberg 1, 14476 Golm, Germany*

⁴*Center for Gravitational Physics and Geometry, Penn State University, University Park, Pennsylvania 16802, USA*

(Received 21 December 2005; published 30 March 2006)

We present a detailed analysis of binary black hole evolutions in the last orbit and demonstrate consistent and convergent results for the trajectories of the individual bodies. The gauge choice can significantly affect the overall accuracy of the evolution. It is possible to reconcile certain gauge-dependent discrepancies by examining the convergence limit. We illustrate these results using an initial data set recently evolved by Brüggmann *et al.* [Phys. Rev. Lett. **92**, 211101 (2004)]. For our highest resolution and most accurate gauge, we estimate the duration of this data set's last orbit to be approximately $59M_{\text{ADM}}$.

DOI: [10.1103/PhysRevLett.96.121101](https://doi.org/10.1103/PhysRevLett.96.121101)

PACS numbers: 04.25.Dm, 04.30.Db, 04.70.Bw, 95.30.Sf

Introduction.—Over the course of the next decade, instruments capable of detecting gravitational radiation (such as LIGO, VIRGO, TAMA, GEO600) are expected to open a new observational window on the Universe. The collision of binary compact objects such as black holes (BHs) is one of the most promising sources for first generation gravitational wave observatories. The theoretical framework for modeling binary BH (BBH) systems is the complete set of nonlinear Einstein equations. Intensive efforts to develop numerical codes able to solve these equations using supercomputers have shown that it is now possible to evolve BHs for periods of an orbit [1–3]. If these simulations are to produce waveforms useful for detector searches, high demands are placed on their accuracy [4].

The near-zone dynamics of binary BH systems are notoriously difficult to simulate and to analyze. Using the Baumgarte-Shapiro-Shibata-Nakamura (BSSN) formulation and a particular set of gauges, a series of BBH configurations, corresponding to initial data in quasicircular orbit at successively larger separations [5], were all found to coalesce in slightly more than a half orbit [2]. A similar BSSN evolution carried out using somewhat different gauges and numerical methods for another data set, slightly further out along the orbital sequence, was found to evolve for much more than the estimated orbital time scale $114M_{\text{ADM}}$ without finding a common apparent horizon (AH) [1]. In fact, no common horizon was found long after the BHs would reasonably be expected to have merged.

In this Letter, we carry out an evolution of the same data set and show that it does, indeed, carry out a complete orbit before a common AH forms. As the BH separation decreases, a local measure of the angular velocity Ω increases, so that the duration of the final orbit is approximately $59M$. The trajectories are convergent for a range of resolutions and within a class of gauge conditions.

However, we do find that very high resolutions are required in order to obtain evolutions close to the contin-

uum limit. The resolutions we have applied here are significantly higher than those used in analogous BH evolutions to date, except for Ref. [3], where similar resolutions were used. With insufficient resolution, we show that it is possible to substantially under- or overpredict the orbital period. We also find that apparently small deviations in the chosen coordinate conditions (gauge), based on the choice of parameters within a particular family, can have a strong influence on the discretization error within the subsequent evolution.

Methods.—Initial data for the evolutions discussed in this Letter correspond to Brandt-Brüggmann “punctures” [6]. The particular orbital parameters are chosen to be identical to those first evolved in Ref. [1], namely, initial separation $L/M = 9.32M$, bare masses $m = 0.47656M$ of each BH, and equal and opposite linear momenta $p = \pm 0.13808$. These parameters are chosen to approximate a BH pair in quasicircular orbit. The angular velocity $\Omega_0 = 0.054988$ suggests an orbital time scale of $114M$ for a perfectly circular orbit. The initial geometry is determined by numerically solving the constraint equations using the solver of Ansorg *et al.* [7].

The binary BH evolution is carried out using the “BSSN” formulation of the Einstein equations [8–10], with an implementation described explicitly in Ref. [11]. We use a version of the “1 + log” lapse and Γ -driver shifts, given by Eqs. (33) [with $f(\alpha) = 2\Psi_{\text{BL}}^m/\alpha$] and (46) [with $F(\alpha) = 3/4\alpha^p/\Psi_{\text{BL}}^n$] of Ref. [11]. We generalize the parameter η to a lapse-dependent coefficient $\alpha^q\eta$, where typically $q \in [0, 4]$. This is helpful for long-term evolution of BHs from large initial separations through merger and will be discussed in detail elsewhere.

We also dynamically adapt our gauges to the horizon location so as to approximate comotion. Individual horizons are located often during the evolution using the finder described in Ref. [12]. From the motion of the horizon centroid, the angular and radial positions and velocities are

determined. Using a damped harmonic oscillator equation, the acceleration needed to bring the horizon centroid back to the initial position is determined by

$$\ddot{\lambda} = -[2TQ\dot{\lambda} + (\lambda - \lambda^0)]/T^2. \quad (1)$$

Here λ stands for either the current azimuthal angle ϕ or radius $r = \sqrt{x^2 + y^2}$ in the orbital plane and λ^0 for its initial value. T and Q are constants determining the time scale and damping factor of the harmonic oscillator. The correction is added to the time derivative of the shift vector as

$$\Delta\dot{\beta}^i = (-y, x, 0)^i\ddot{\theta} - (x, y, 0)^i\dot{r}/r^0. \quad (2)$$

The punctures are excised using an extension of the “simple excision” techniques which have proven successful in evolving single BH spacetimes [13,14]. In particular, we apply the boundary condition to an embedded boundary whose shape is determined by the horizon location, as described in Refs. [2,15].

Spatial differentiation is performed via straightforward finite-differencing, incorporating nested mesh-refined grids with the highest resolution concentrated in the neighborhood of the individual horizons. The mesh refinement is implemented via the carpet driver [16] for CACTUS. The evolutions carried out in this Letter made use of 8 levels of fixed 2:1 refinement. We fix the regions of increased resolution around the initial BH locations. Because we are making use of a BH-adapted gauge, the individual horizons remain on the fine grids throughout the evolution without requiring moving grids or excised regions. We have used

finest grid resolutions of $h = 0.025M$, $0.02M$, $0.018M$, $0.015M$, and $0.0125M$, with an outer boundary at $96M$ in all cases. Our overall finite-differencing accuracy is second order in space and time.

As a diagnostic of the dynamics of the individual BHs, we measure the proper distance within a slice between the pair of AHs. This is calculated by shooting spacelike geodesics from the origin (taking advantage of the spacetime symmetry) to one of the horizon surfaces [17]. As this measure of distance is within each slice, it does depend on the particular lapse condition (as will be seen below) but still provides useful information about the near-zone BH motion in the given slicing.

Results.—Evolutions were carried out for a number of resolutions and gauge parameters. A first observation, important in interpreting the results of Refs. [1,2], is that the infall coordinate trajectory at a given resolution depends crucially on the gauge choice. In Fig. 1, the results of evolutions of three choices of gauge parameters (introduced above) are displayed. The first, which we label “GC1,” sets $(m, n, p, q, \eta, T, Q) = (0, 2, 1, 1, 4, 5, 1)$. The second gauge choice “GC2” sets parameters to $(4, 2, 1, 4, 2, 5, 1)$. The third gauge choice “GC3” is described below. Plotted are the proper separations of the AHs within the slice versus the coordinate time.

We note that, for the GC1 evolutions at a grid spacing of $h = 0.025M$, the BHs fall together rather rapidly. By coordinate time $t = 75M$, the proper distance between the AHs is down to $L/M = 4.5$. Increasing the resolution to $h = 0.020M$, $h = 0.018M$, and $h = 0.015M$, there is a trend towards longer evolution times before reaching the same separation, though the convergence is slow. For the highest resolution which we have evolved, $h = 0.0125M$, the infall to the same separation is delayed to only $t = 88M$.

The evolutions resulting from gauge choice GC2 have an entirely different character. At the lowest resolution, with $h = 0.025M$, we find that not only does the system evolve well beyond an orbital time period before a common AH appears, the orbit appears to be elliptical, with proper separation first increasing with time, and then falling back, reaching a separation $L/M = 4.5$ only after $t = 119M$. This behavior is qualitatively similar to what was reported for the same initial data set in Ref. [1]. Increasing the resolution as above, however, we find a faster coalescence as resolution is increased, and the apparent elliptical nature of the orbit disappears.

Importantly, the two families of evolutions corresponding to GC1 and GC2 do show a tendency towards each other as resolution is increased. In fact, a 3-term Richardson extrapolation (eliminating 2nd and 3rd order error terms) of the computed trajectories show that the two families converge to a common result in the continuum limit. Figure 1 also shows the results of the extrapolation for both sets of evolutions at the 3 highest resolutions where we had sufficient data available. (Using other sets of 3 resolutions gives very similar results.)

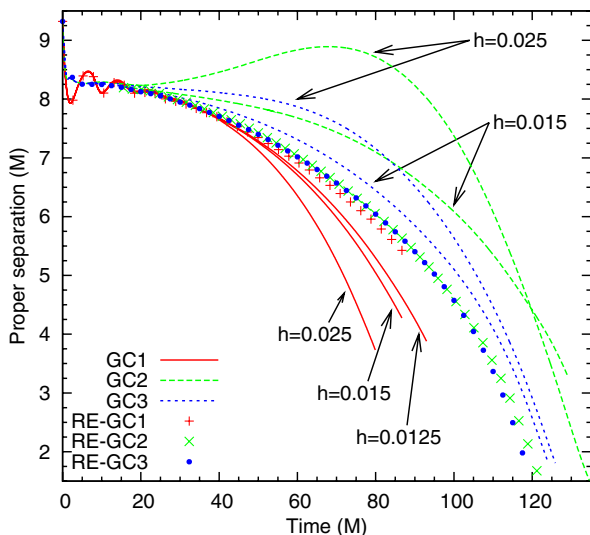


FIG. 1 (color online). The minimal proper distance between individual AHs as a function of time. Lines show two representative resolutions $h = 0.025M$ and $h = 0.015M$ for each gauge choice GC1, GC2, and GC3 discussed in the text and an $h = 0.0125M$ evolution for GC1. Points show Richardson extrapolations (RE) for resolutions $h \in \{0.018, 0.015, 0.0125\}M$ for GC1, $h \in \{0.020, 0.018, 0.015\}M$ for GC2, and $h \in \{0.025, 0.020, 0.015\}M$ for GC3.

The differences between GC1 and GC2 results may at first seem to be the expected result of the variation in slicing condition between the two classes of evolutions. However, the fact that the results converge to the same coordinate trajectory in the continuum limit suggests a somewhat different explanation, namely, that the finite difference error inherent in the evolution (particularly in the lapse) can be strongly influenced by the gauge choice.

The Richardson extrapolation provides an indication of the accuracy of the evolutions at a given resolution or, conversely, the resolution required to obtain a result of a given accuracy. The Richardson-extrapolated coordinate trajectory seems robust, but we note that the highest resolution ($h = 0.0125M$) GC2 simulations which we have carried out still represent a 22% error in separation at $t = 100M$ compared to the extrapolated result. The sensitive dependence of accuracy on gauge suggests that “ideal” gauge conditions may be able to improve the accuracy greatly at a given resolution.

Based on results of the previous experiments, a third gauge choice parameter was found to demonstrate this point. Under the label GC3, evolutions of the same data were carried out using gauge parameters (4, 2, 1, 4, 2, 5, 2.6), i.e., the same as for GC2 except for the drift-correction damping parameter. The GC3 results are also plotted in Fig. 1. Once again, we find the proper separation measure to be convergent with increasing resolution and, further, that the Richardson extrapolation lies on top of the curves predicted by the previous evolutions. However, in this case the highest resolution attempted, $h = 0.015M$, lies much closer to the limiting trajectory.

Figure 2 plots the evolution of the individual BHs’ angular velocity, as measured by the AH centroid’s drift, for GC3 at our highest evolved resolution. From our experience with more closely separated binaries, the initial shift profile corresponded to a quasirigid rotation with $\Omega = 0.3$, approximately 60% of the nominal $\Omega_0 = 0.055$ of the

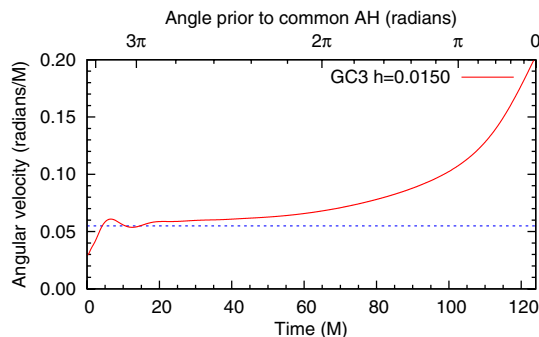


FIG. 2 (color online). Angular motion of individual AHs as a function of time (lower scale) and angle (upper scale, in radians measured backwards along the orbit from the first appearance of a common AH). The curve shows the angular velocity Ω of the AH centroid for GC3, as measured by integrating the corrections applied to the gauge via (1). The horizontal line corresponds to the $\Omega_0 = 0.055$ estimated for the initial data.

initial data [18]. The corotation shift adjustment (1) quickly raises the effective angular velocity of the coordinate system up to a value close to the initial data prediction Ω_0 . As expected, this angular velocity then gradually increases as the BHs spiral together.

Figure 3 plots the overall motions of the AHs for the same GC3 case as Fig. 2. The individual horizon shapes are shown at intervals of $5M$, transformed according to the radial and angular motion determined above. The initial rapid dip in separation from $9.32M$ to $8.3M$ in Fig. 1 can now be seen to be largely a result of the initial coordinate expansion of the individual horizons, due to our choice of zero radial shift in the initial data.

A common AH is first detected at $t = 124M$, by which time an angular displacement of 10.2 radians, or 1.6 revolutions, has taken place. The common horizon is found via the method of pretracking, in which a family of surfaces with the smallest possible generalized expansion is followed to provide an estimate which converges on the first common AH [19]. The listed time is expected to correspond to the first genuine appearance of a common AH, independent of the search algorithm. Counting backwards from the appearance of the common horizon, the duration of the last orbit is approximately $59M$. It is interesting to note that, for the cases where a common horizon is found, it occurs when the proper separation is approximately $1.8M$. Our Richardson-extrapolated GC1 and GC2 evolutions reach this same separation less than $5M$ earlier than this GC3 evolution.

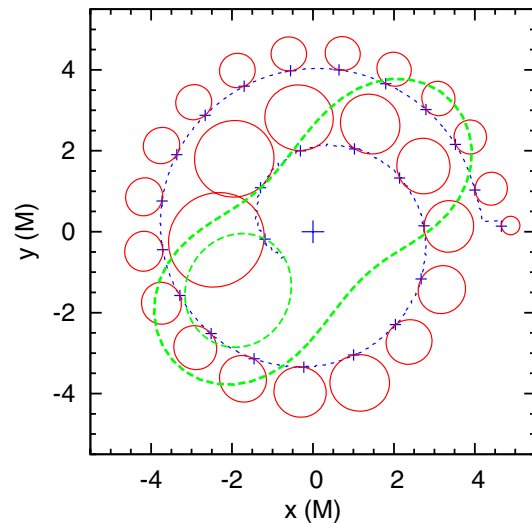


FIG. 3 (color online). Schematic showing the motion of one of the BHs with time, for the GC3 gauge choice at the highest resolution $h = 0.015M$. At intervals of $t = 5M$, the AH cross sections in the xy plane are plotted by transforming the corotating coordinate system by the specified angle and distance. The apparent growth of the AHs with time is a nonphysical coordinate effect. The first appearance of a common AH at $t = 124M$ and the corresponding final single AH are shown superposed on the figure as dotted lines.

Given the demonstrated resolution dependence of these results, it is likely that these results will be subject to some modification as more accurate evolutions become available. It should also be recalled that a merged event horizon within the slice will have formed earlier than the common AH. Experience with closely separated binaries suggests that this is typically not more than about $5M$ before the appearance of the first common AH, but studies of the event horizon evolution for these spacetimes will need to be the subject of future studies. We also note that the notion of an “orbit” for closely separated BHs is an intrinsically gauge-dependent quantity—for example, a sufficiently small lapse in the region of the horizons could be used to indefinitely delay merger. The slicings used here are quite similar in profile to maximal slices and, thus, not atypical for numerical relativity simulations.

As a final point, we note that a number of measures of accuracy have been monitored during the course of these evolutions. In particular, the constraint violation is found to remain below a value of 0.05 at all points outside the BH horizons and away from the boundaries for the duration of the runs. The AH masses of the individual BHs were measured and found to be essentially constant, convergent, and accurate even for the low resolution runs. We have also compared binaries with closer separation, such as the “QC-0” data evolved by a number of groups [2,20,21] and find excellent agreement with published results.

Conclusions.—We have carried out evolutions of BBH configurations, from initial data in quasicircular orbit, through plunge, to the formation of a common horizon. The dynamics exhibit a number of interesting properties.

Using a measure of angular velocity based on the AH motion, we have found that the black holes remain separated for more than 1.5 revolutions. This measure initially yields an angular velocity which is consistent with the initial data model. The most accurate estimate of the duration of the last complete orbit before formation of the first common AH was $59M$. As might be expected for bodies falling towards each other, this orbital period is considerably less than is predicted by the initial angular velocity, $114M$. The results have been carried out at resolutions much higher than similar studies to date and exhibit good numerical consistency under a range of resolutions and for a variety of gauge parameter choices.

By Richardson extrapolating the black hole trajectories, we derived what appears to be a robust estimate of their continuum limit, which proved to be almost independent of gauge choice, at least within the family of gauges considered here.

These evolutions required extremely high resolution to attain good accuracy. Insufficient resolution can result in very different predictions for the orbital trajectories and the period of the final orbit. This period directly influences the phase of asymptotically observed waveforms at their strongest point and, thus, is crucial to reproduce accurately.

We demonstrated that the gauge choice can feed directly into the numerical accuracy of the solution, due to un-

wanted dynamics in the evolution variables caused by gauge effects. A preferred gauge was found to significantly improve the accuracy at a given resolution. A more detailed exposition of the gauge conditions used here, applied to a sequence of initial data configurations, will be the subject of upcoming studies.

We thank B. Brügmann for many discussions and for sharing details of his codes, M. Ansorg for providing the initial data solver, and L. Rezzolla and M. Alcubierre for many discussions and suggestions. We have used computing time allocations at the AEI, CCT, LRZ, NCSA, NERSC, PSC and RZG. We use the CACTUS code infrastructure with a number of locally developed thorns. This work was supported in part by DFG Grant No. SFB TR/7 “Gravitational Wave Astronomy,” by the Center for Computation and Technology at LSU, and the Center for Gravitational Wave Physics at PSU.

-
- [1] B. Brügmann, W. Tichy, and N. Jansen, Phys. Rev. Lett. **92**, 211101 (2004).
 - [2] M. Alcubierre, B. Brügmann, P. Diener, F.S. Guzmán, I. Hawke, S. Hawley, F. Herrmann, M. Koppitz, D. Pollney, E. Seidel, and J. Thornburg, Phys. Rev. D **72**, 044004 (2005).
 - [3] F. Pretorius, Phys. Rev. Lett. **95**, 121101 (2005).
 - [4] M. Miller, Phys. Rev. D **71**, 104016 (2005).
 - [5] G.B. Cook, Phys. Rev. D **50**, 5025 (1994).
 - [6] S. Brandt and B. Brügmann, Phys. Rev. Lett. **78**, 3606 (1997).
 - [7] M. Ansorg, B. Brügmann, and W. Tichy, Phys. Rev. D **70**, 064011 (2004).
 - [8] T. Nakamura, K. Oohara, and Y. Kojima, Prog. Theor. Phys. Suppl. **90**, 1 (1987).
 - [9] M. Shibata and T. Nakamura, Phys. Rev. D **52**, 5428 (1995).
 - [10] T.W. Baumgarte and S.L. Shapiro, Phys. Rev. D **59**, 024007 (1999).
 - [11] M. Alcubierre, B. Brügmann, P. Diener, M. Koppitz, D. Pollney, E. Seidel, and R. Takahashi, Phys. Rev. D **67**, 084023 (2003).
 - [12] J. Thornburg, Classical Quantum Gravity **21**, 743 (2004).
 - [13] M. Alcubierre and B. Brügmann, Phys. Rev. D **63**, 104006 (2001).
 - [14] M. Alcubierre, B. Brügmann, D. Pollney, E. Seidel, and R. Takahashi, Phys. Rev. D **64**, 061501(R) (2001).
 - [15] M. Alcubierre, B. Brügmann, P. Diener, F. Herrmann, D. Pollney, E. Seidel, and R. Takahashi, gr-qc/0411137.
 - [16] E. Schnetter, S.H. Hawley, and I. Hawke, Classical Quantum Gravity **21**, 1465 (2004).
 - [17] M. Koppitz, Ph.D. thesis, University of Potsdam, 2004.
 - [18] W. Tichy and B. Brügmann, Phys. Rev. D **69**, 024006 (2004).
 - [19] E. Schnetter, F. Herrmann, and D. Pollney, Phys. Rev. D **71**, 044033 (2005).
 - [20] M. Campanelli, C.O. Lousto, P. Marronetti, and Y. Zlochower, gr-qc/0511048.
 - [21] J.G. Baker, J. Centrella, D.-I. Choi, M. Koppitz, and J. van Meter, gr-qc/0511103.